Expert Systems with Applications 36 (2009) 3845–3856

Contents lists available at ScienceDirect

Expert Systems with Applications

journal homepage: www.elsevier.com/locate/eswa

Stitching defect detection and classification using wavelet transform and BP neural network

W.K. Wong [a,*], C.W.M. Yuen [a], D.D. Fan [a], L.K. Chan [a], E.H.K. Fung [b]

[a] Institute of Textiles and Clothing, The Hong Kong Polytechnic University, Hunghom, Kowloon, Hong Kong
[b] Department of Mechanical Engineering, The Hong Kong Polytechnic University, Hunghom, Kowloon, Hong Kong

ARTICLE INFO

Keywords:
Stitching defect
Image segmentation
Defect classification
Wavelet transform
Quadrant mean filter
Neural network

ABSTRACT

In the textile and clothing industry, much research has been conducted on fabric defect automatic detection and classification. However, little research has been done to evaluate specifically the stitching defects of a garment. In this study, a stitching detection and classification technique is presented, which combines the improved thresholding method based on the wavelet transform with the back propagation (BP) neural network. The smooth subimage at a certain resolution level using the pyramid wavelet transform was obtained. The study uses the direct thresholding method, which is based on wavelet transform smooth subimages from the use of a quadrant mean filtering method, to attenuate the texture background and preserve the anomalies. The images are then segmented by thresholding processing and noise filtering. Nine characteristic variables based on the spectral measure of the binary images were collected and input into a BP neural network to classify the sample images. The classification results demonstrate that the proposed method can identify five classes of stitching defects effectively. Comparisons of the proposed new direct thresholding method with the direct thresholding method based on the wavelet transform detailed subimages and the automatic band selection for wavelet reconstruction method were made and the experimental results show that the proposed method outperforms the other two approaches.

1. Introduction

Detection of defects plays an important role in the automated inspection of fabrics and garment products. Quality inspection of garment manufacturing still relies heavily on trained and experienced personnel checking semi-finished and finished garments visually. However, manual inspection imposes limitations on identifying defects in terms of accuracy, consistency and efficiency, as workers are subject to fatigue or boredom and thus inaccurate, uncertain and biased inspection results are often produced. As a result, garment inspection is highly prone to errors and it allows defects to go undetected. To tackle these problems, it is necessary to set up an advanced inspection system for garment checking that can decrease or even eliminate the demand for manual inspection and increase product quality.

In automated inspection, it is necessary to solve the problem of detecting small defects that locally break the homogeneity of a texture pattern and to classify all different kinds of defects. Various techniques have been developed for fabric defect inspection. Most of the defect detection algorithms tackling the problem use Gaussian Markov random field, the Fourier transform, the Gabor filters or the wavelet transform.

Cohen, Fan, and Attai (1991), Gupta and Sortrakul (1998) and Pyun et al. (2007) used a model-based method such as Gaussian Markov random field to inspect fabric defects and the method is computationally intensive. Fourier-based methods characterize the spatial-frequency distribution of images, but they do not consider the information in the spatial domain and may ignore local deviations (Chan & Pang, 2000; Tsai & Huang, 2003; Zhang & Bresee, 1995). The Artificial Neural Network (ANN) was developed to assess set marks but the parameter selection was inadequate and the results were unsatisfactory (Vangheluwe, Sette, & Pynckels, 1993). In 1996, Tsai and Hu (1996) classified the inputs of nine parameters obtained from a fabric image's Fourier spectrum using the BP neural network. Nevertheless, the identification rate was not satisfactory. Gabor filters have been recognized as a joint spatial/spatial-frequency representation for analyzing textured images and detecting defects that contain highly specific frequency and orientation characteristics (Bovik & Clark, 1990; Coggins & Jain, 1989; Jain & Farrokhnia, 1991). A potential disadvantage of the decomposition of the Garbor filters is that they are computationally intensive. The Gabor filter banks are not mutually orthogonal, which may result in a significant correlation among texture features obtained from the Gabor-filtered images. Wavelet

* Corresponding author.
E-mail address: tcwongca@inet.polyu.edu.hk (W.K. Wong).

0957-4174/$ - see front matter © 2008 Published by Elsevier Ltd.
doi:10.1016/j.eswa.2008.02.066

transform has become a popular alternative for fabric defect detection. The use of a pyramid-structured wavelet transform for texture analysis was first suggested in the pioneering work of Mallat (1989). This initial technique has been improved by several studies on texture detection and classification (Chang & Kuo, 1993; Lu, Chung, & Chen, 1997; Unser, 1995).

Unser (1995) found that texture features were concentrated on the intermediate frequency band and they proposed a multiresolution method based on a tree-structured wavelet transform for fabric texture analysis and classification. Lu et al. (1997) suggested that the intra-scale and inter-scale fusion schemes for unsupervised texture segmentation, correlation or dependency between scales should be taken into account to attain satisfactory texture classification and segmentation. Texture features extracted from wavelet-decomposed images were widely used for fabric defect detection (Chitre & Dhawan, 1999; Song, Chen, Wen, & Ge, 2003; Yang, Pang, & Yung, 2002, 2004). Many other methods not relying on texture features have been proposed (Ngan, Pang, Yung, & Ng, 2005; Sari-Saraf & Goddard, 1999; Tsai & Chiang, 2003). The combination of wavelet transform techniques with other methods such as the co-occurrence matrix techniques (Amet, Ertuzun, & Ercil, 1998; Arivazhagan & Ganesan, 2003), fuzzy inferencing (Dorrity, Vachtsevanos, & Jasper, 1996), generic algorithms (Jasper, Joines, & Brenzovich, 2005), the Gaussian mixture model-based classifier (Kim & Kang, 2007) and ANFIS classifier (Sengur et al., 2007) was also proposed for defect detection and classification.

Little research has been carried out to detect and classify fabric stitching. The quality of fabric stitching is one of the key factors to determine the quality of a garment. In the apparel industry, identifying the quality of fabric stitching through human inspection is not reliable. The stitches of garments are thin surface anomalies embedded in homogeneously structural and statistical textures. In order to detect and classify stitching defects, it is necessary to segment them from the texture background accurately. The textural analysis methods based on the extraction of texture features in the spatial and spectral domains result in high dimensionality (Tsai & Chiang, 2003). Although the methods not relying on textual features are successfully applied to thick fabric defect detection (Ngan et al., 2005; Sari-Saraf & Goddard, 1999; Tsai & Chiang, 2003), they are not effective in the thin surface anomalies. The aim of this research is to develop an effective way to detect and classify defects in stitches of fabric. The proposed approach is based on a multiresolution representation of the wavelet transform with the stages of image smoothing, thresholding and noise filtering. For further improvement of the performance, this study uses the direct thresholding method, which is based on wavelet transform detailed subimages from the use of a quadrant mean filtering method, to attenuate the texture background and preserve the anomalies. After the binary image is obtained, the BP neural network is used to classify the stitching defects.

The remainder of this paper is organized as follows. Section 2 gives a literature review of previous fabric defect detection methods. In Section 3, four segmentation stages including wavelet decomposition, image smoothing, thresholding and noise filtering are described and the feature extraction module and the method of classifying stitching defects are demonstrated. Section 4 presents the experimental results of a variety of stitching defects. Finally, conclusions are given in Section 5.

2. Literature review

Wavelet transform has been developed for over 20 years. It is a multiresolution technique which can be implemented as a pyramid or a tree structure and is similar to subband decomposition. A wavelet decomposition can be performed by a pyramidal algorithm in which a pair of wavelet filters including a low-pass filter and a high-pass filter are utilized to calculate wavelet coefficients (Mallat, 1989, 1999). With the pyramid-structured wavelet transform, the original image first passes through the low-pass and high-pass decomposition filters to generate four lower resolution components: one low–low (LL) subimage, which is the approximation of the original image and is also called smooth image, and three detailed subimages, which represent the horizontal, vertical, and diagonal directions of the original image. The decompositions are repeated on the LL subimage to obtain the next four subimages. Fig. 1 shows the 2-scale wavelet decompositions. The energy content of the low–low band is above 95%.

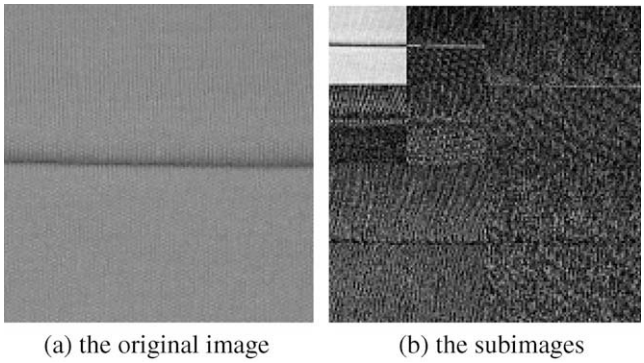

Fig. 1. Pyramid-structured wavelet transform.

Two categories of fabric defect detection based on wavelet transform are found in the literature. One category is the direct thresholding method (Ngan et al., 2005; Tsai & Chiang, 2003) whose design is based on the fact that texture background can be attenuated by the wavelet decomposition. Textural features extracted from wavelet-decomposed images are another category which is widely used for fabric defect detection. Wavelet transform is able to characterize effectively the essential differences between textures (Mallat, 1999) and therefore is widely applied to detect defects. These two methods are introduced below.

2.1. Textural features extracted from wavelet-decomposed images

Textural features extracted from wavelet-decomposed images have been used for texture classification and segmentation (Chitre & Dhawan, 1999; Song et al., 2003) and applied to fabric defect detection (Amet et al., 1998; Arivazhagan & Ganesan, 2003; Kim & Kang, 2007; Sengur et al., 2007; Yang et al., 2002, Yang, Pang, & Yung, 2004). Yang et al. (2002) proposed a method of fabric defect classification by incorporating the design of a wavelet frames-based feature extractor into the design of a Euclidean distance-based classifier. Yang also compared six wavelet transform-based classification methods, using different discriminative training approaches to the design of the feature extractor and the classifier (Yang et al., 2004). Amet et al. (1998) proposed a method based on the subband decomposition of gray level images through wavelet filters and the extraction of the co-occurrence features from the subband images to detect fabric defects. Arivazhagan and Ganesan (2003) presented a texture segmentation algorithm based on the wavelet decomposition of images, and statistical features were extracted from the subband images using co-occurrence matrix techniques. Kim and Kang (2007) applied the wavelet packet frame decomposition to capture the dominant texture features and proposed the Gaussian mixture model-based classifier to assign each pixel to the class. This method was also successfully applied to fabric defect detection. Sengur et al. (2007) proposed a texture classification algorithm based on the wavelet domain feature extractor and an ANFIS classifier.

However, the texture analysis method based on the extraction of textural features in the spatial and spectral domains results in high dimensionality. The method requires sophisticated classifiers to discriminate textural variations. The most difficult task of the feature extraction approach is to choose adequate textural features which can sufficiently represent the uniqueness of the texture of the image. A set of features that are the optimal representation of a specific texture could be completely useless for other textures (Tsai & Chiang, 2003).

2.2. Method of direct thresholding on wavelet transform subimages

2.2.1. Automatic band selection for wavelet reconstruction in the application of defect detection

Apart from the methods based on the textural features extracted from wavelet-decomposed images, other methods have also been proposed (Ngan et al., 2005; Sari-Saraf & Goddard, 1999; Tsai & Chiang, 2003). Tsai and Chiang (2003) proposed an image reconstruction approach based on an efficient image restoration scheme using wavelet transform for inspecting defects. By properly selecting the smooth subimage or the combination of detailed subimages at different resolution levels and binarizing the selected subimage, the surface defects are well detected. For statistical textures with isotropic patterns or structural textures containing all horizontal, vertical and diagonal orientations, the smooth subimage is included in the reconstruction process to enhance the defects in the restored image. For structural textures with high directionality, the selective detailed subimages are included in the reconstruction process to remove all repetitive and oriented textures. As most fabrics show a structural texture containing all horizontal, vertical and diagonal orientations, the smooth subimage is included in the reconstruction process.

The l_2-norm is used as the energy function to identify dominant frequency subbands of a textured pattern. J denotes the total number of decomposition levels. W^j, W^j_H, W^j_V, W^j_D represent the decomposition results LL, LH, HL and HH at scale j, respectively. For J-scale decompositions, the original signal is represented by $(W^J, (W^j_H, W^j_V, W^j_D)_{1\leqslant j\leqslant J})$, where the size of the wavelet representation is the same as that of the original signal. This representation is composed of a coarse signal at resolution J and a set of detailed signals at resolutions $1 \sim j$.

The energy of the smooth subimage at level J is given by

$$E^j_s = \sum_x \sum_y [W^j(x,y)]^2 \tag{1}$$

E^j_h, E^j_v, E^j_d represent the energy of the other three detailed subimages at level j. The equation is similar to (1).

The total energy of the image in J multiresolution levels is given by

$$E = E^J_s + \sum_{j=1}^{J} E^j_h + \sum_{j=1}^{J} E^j_v + \sum_{j=1}^{J} E^j_d. \tag{2}$$

The choice of a proper number of multiresolution levels is based on the energy ratio of detailed subimages at two consecutive levels. D_j denotes the normalized energy sum of the three detailed subimages at resolution level j, i.e.

$$D_j = (E^j_h + E^j_v + E^j_d)/E. \tag{3}$$

The energy ratio of detailed subimages between resolution levels j and $j-1$ is given by

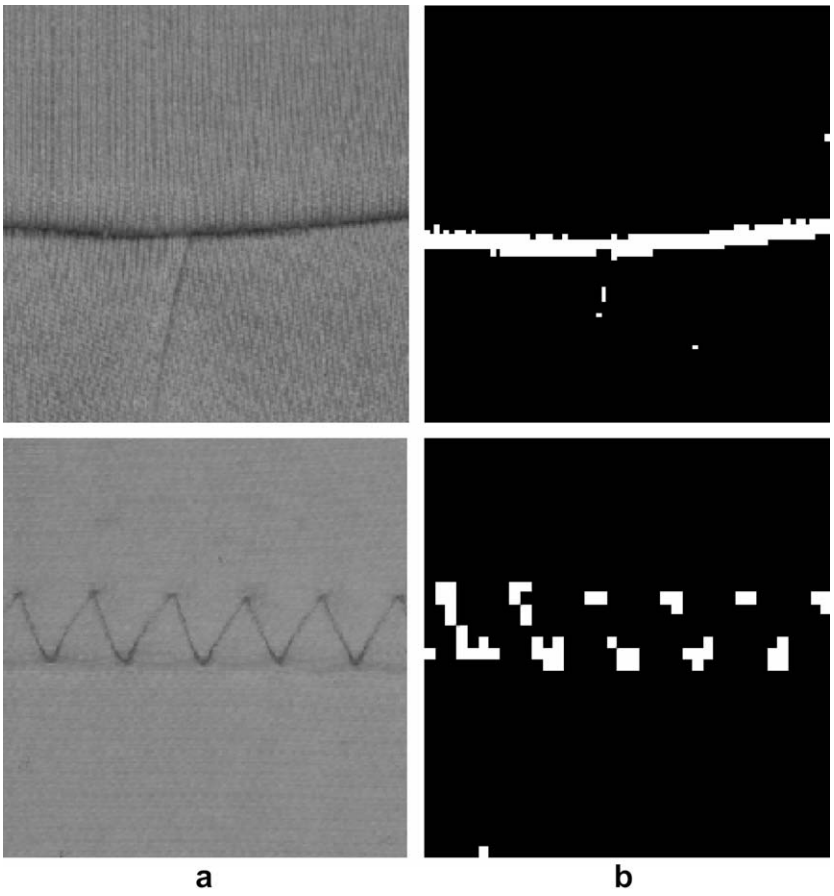

Fig. 2. (a) Stitching image and (b) binarized images using the automatic band selection for the wavelet reconstruction method.

Table 1
The energy ratio of Fig. 2a

Resolution level	D_j	R_j
1	0.0010	–
2	0.0015	1.5193
3	0.0016	1.0898
4	0.0019	1.1803

$$R_j = \frac{D_j}{D_{j-1}}, \quad j = 2, \ldots, J. \tag{4}$$

The best number of resolution level J^* is chosen when R^j is a minimum, i.e.

$$J^* = \min_j \{R_j\}. \tag{5}$$

The total number of the decomposition level was set as $J = 4$. Fig. 2 shows the results of the automatic band selection for the wavelet reconstruction method. The fabric stitching of the two original images cannot be fully detected and a large portion of the stitching regions cannot be covered even in the lower image. Table 1 lists the statistics of D_j (the normalized energy sum of the three detailed subimages) and R_j (the energy ratio of detailed subimages). It shows that R_j reaches the minimum at resolution level $j = 3$. The corresponding level of Fig. 2b is 4. After being tested for many times, the automatic selected level was found to be so high that the stitching defects could not be outlined clearly. The automatic band selection for the wavelet reconstruction method is not effective for tackling the fabric stitching detection problem and there is still much room for improvement.

2.2.2. Direct thresholding based on wavelet transform detailed subimages

Ngan et al. (2005) proposed the direct thresholding method based on wavelet transform for defect detection. The proposed stages of the method are illustrated as follows:

Step 1: Use the reference images for Haar wavelet decomposition.
Step 2: Extract the corresponding fourth-level horizontal and vertical details.
Step 3: Obtain the lower and upper bounds among all pixel values of each detailed image for the threshold values.
Step 4: In order to reduce the noise, the threshold values should be $[0.97^* t_{\text{lower},i}, 0.97^* t_{\text{upper},i}]$ for each detail i.
Step 5: Average the lower and upper bound values of the three horizontal details at level 4 and repeat the process for vertical details.
Step 6: Use the average values to threshold the detailed images at level 4.
Step 7: Perform an Or-operation of horizontal and vertical details at level 4.
Step 8: Apply the smoothing filter and remove the noise after the or-operation.

To evaluate the direct thresholding method of fabric stitching detection, 30 samples for each kind of fabric stitching image (Fig. 3) were used. Fig. 3 gives the results of the direct thresholding method based on wavelet transform. The stitches in the upper image was detected better than the stitches in the lower image. On the one hand, the larger decomposition levels generated coarser representation of the stitching, but on the other hand the main

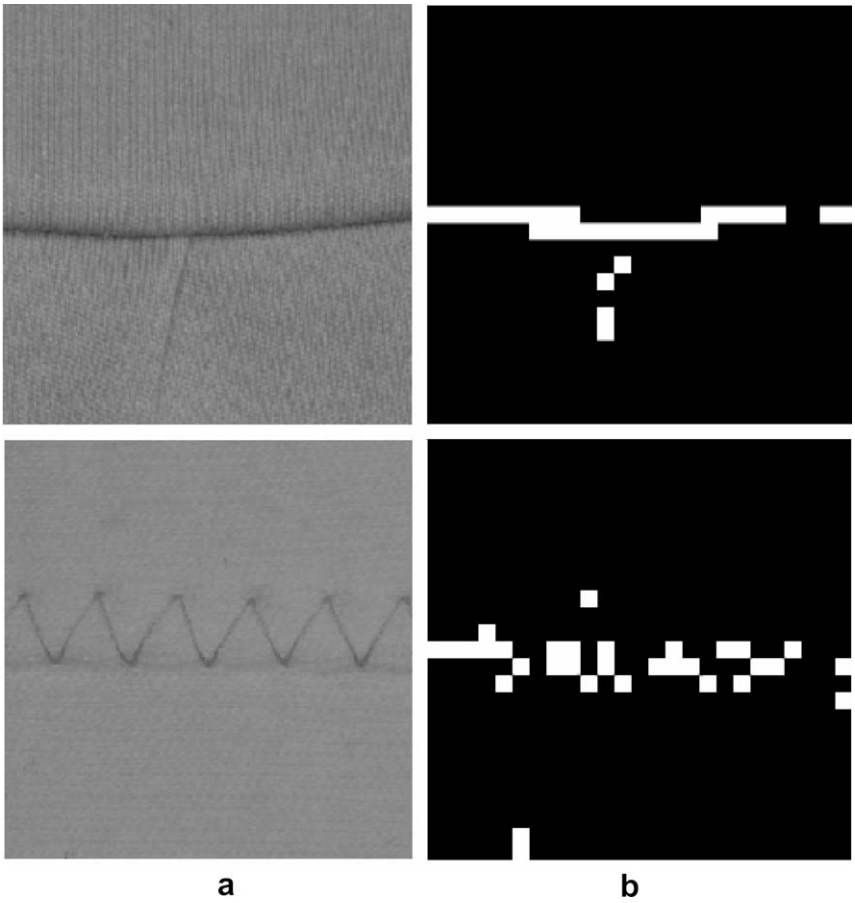

Fig. 3. (a) Stitching image and (b) thresholded images using direct thresholding method based on wavelet transform.

energies were concentrated on the low frequency subband, and therefore the fusion of the horizontal and vertical subimages cannot yield satisfactory results. The method cannot outline the shape of the stitches adequately.

3. Stitching defect detection and classification method using wavelet transform and BP neural network

Five classes of common stitching defect samples, namely pleats, puckers, tension, skipped-stitches and holes, are analyzed in this study as shown in Fig. 4. To design the stitching defect segmentation algorithm, the images of fabrics constituting ordered textures are globally homogenous. In other words, statistics measured from different patches in an image are correlated. It is further noted that images containing stitches are less homogenous than the defect-free ones. The essence of the proposed segmentation algorithm is to localize those defects in the image that disrupt the global homogeneity of the background texture.

Fig. 5 illustrates the flow diagram of the proposed stitching defect detection and classification method. The proposed algorithm consists of a stitching defect segmentation module and a classification module. In the stitching defect segmentation module, the input images are decomposed by wavelet transform at an appropriate resolution level. Then the quadrant mean filter is applied to smooth the image. After thresholding and noise filtering, a binary image can be obtained when the stitching anomalies can be segmented from the fabric texture background. In the classification module as shown in Fig. 5, the feature vectors extracted from the spectral measurement of the binary image are input into the BP neural network to classify the types of sample images.

3.1. Stitching defect segmentation algorithm

3.1.1. Wavelet transform

The wavelet transform module constitutes a step of image segmentation with the objectives of attenuating the background texture and accentuating the anomalies. Through the wavelet decomposition on an appropriate scale, a smooth image, which is a coarse approximation of the original image, and three detailed images, which contain fine structures in horizontal, vertical and diagonal orientations, can be obtained. For the structural textures containing all horizontal, vertical and diagonal orientations, the smooth subimage is used to enhance the defects in the restored image (Tsai & Chiang (2003)). Hence, the smooth subimage is chosen for further image segmentation. The global repetitive texture pattern can be effectively removed and only local anomalies are preserved in the restored image through the image smoothing and thresholding.

The higher resolution level is used and the better uniformity of gray levels can be obtained. However, the higher level of resolution generates the fusion effect for the anomalies and may cause the localization error of the detected stitches Tsai and Chiang (2003). The effect of varying the multiresolution levels of restoration results for stitches of a garment is demonstrated in Fig. 6, which demonstrates that the high resolution level causes the blur of the stitching defect. The determination of a proper multiresolution level is crucial to the success of background-texture removal and defect detection. By selecting an appropriate level, the wavelet transform can show a significant detection result. The texture region is suppressed and the anomaly region is enhanced. In our study, an appropriate level was chosen through observing the output of wavelet decomposition of a large number of images.

Haar wavelet, Daubechies wavelet and Battle–Lemarie wavelet had similar performance in terms of classification of the test samples (Mallat, 1989). Hence, the properties of the wavelets (vanishing moments, size of support and regularity) have limited impact on defect detection and classification. The Daubechies wavelet was employed in the wavelet decomposition in this study.

3.1.2. Image smoothing

A common problem of texture segmentation is the boundary effects. In the smooth subimage, the intensity variation in homogeneous regions is very small whereas the intensity variation in anomaly regions is distinctly large with respect to the entire image. A pixel near the background texture boundary has neighboring

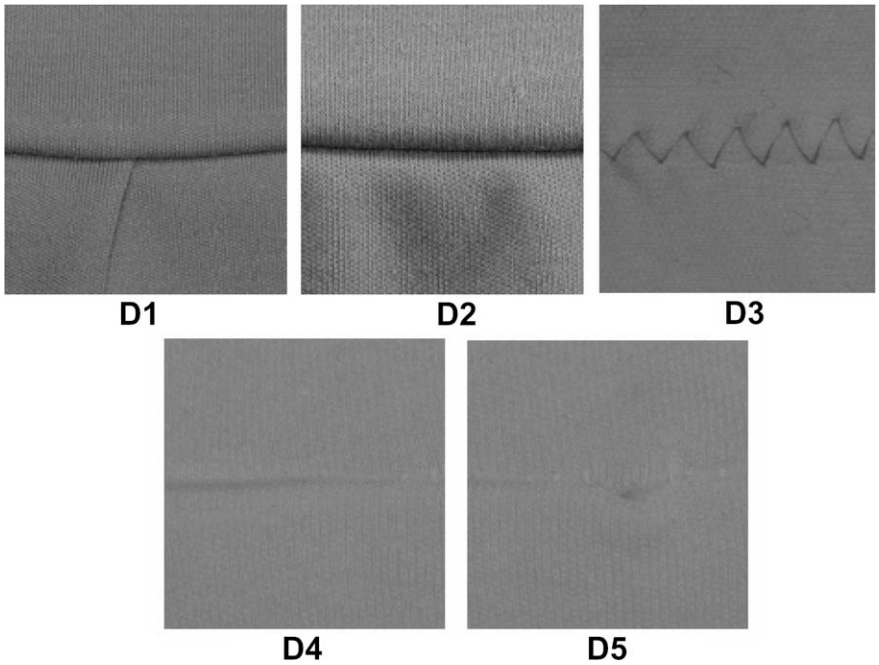

Fig. 4. Five classes of stitching defect samples for experiments: D1 (Pleats), D2 (Puckers), D3 (Tension), D4 (Skipped-stitches) and D5 (Holes).

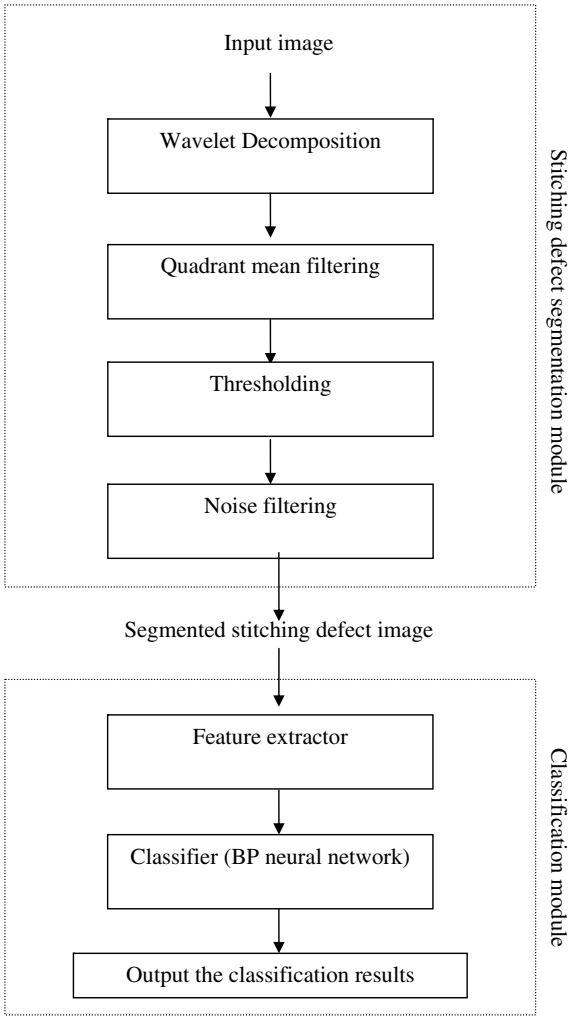

Fig. 5. Block diagram of the stitching defect detection and classification algorithm.

pixels belonging to the anomaly. Hence, it is necessary to further smooth the obtained subimages. The raw images of the selected subbands are filtered using a quadrant mean method which smoothes noise and makes the boundary accurate (Jiang & Sawchuk, 1986; Song et al., 2003).

A general local window centered at pixel (x,y) contains a heterogeneous region. There are difficulties in localizing the boundary in an exact manner. When considering four local windows including a pixel (x,y) (Fig. 7), $W(x,y)$ represents the image and w represents the window size of quadrant variances. The energy mean $m_1(x,y)$ and the energy variance $v_1(x,y)$ of the upper-left window are defined as

$$m_1(x,y) = \frac{1}{w^2}\sum_{i=0}^{w-1}\sum_{j=0}^{w-1}|W(x+i,y-j)| \tag{6}$$

and

$$v_1(x,y) = \frac{1}{w^2}\sum_{i=0}^{w-1}\sum_{j=0}^{w-1}(W(x+i,y-j)-m_1(x,y))^2. \tag{7}$$

The energy mean and the energy variance of the other three windows are similar to Eqs. (6) and (7).

The variance $v(x,y)$ is used to measure the gray level variability around a pixel to find the most homogeneous neighborhood. Accordingly, the energy at a pixel (x,y) is taken as the average of the neighborhood that has the minimum variance among the four local windows. Blurring due to averaging operation across the region boundaries is minimized by choosing the position of the local window with the minimum variance. One important issue of texture segmentation is the choice of an appropriate filter size. Larger filters decrease the exact location of anomalies while smaller filters tend to improve the boundaries localization. In this study, the window size for quadrant variances $w = 2$ was determined by experiments.

3.1.3. Thresholding and noise filtering

Once the improved images are gathered, the next step is to conduct image segmentation. Image thresholding is crucial to applications of image segmentation. In the improved image, the intensity variation in homogeneous regions is very small whereas the intensity variation in defective regions is distinctly large. In order to visualize and localize the stitching defects, the gray-level image needs to be operated by thresholding processing. The binary image has only two values, 0 or 1. Value 1 is used for the pixels of seams or stitching defects while value 0 is used for the pixels of normal texture.

Firstly, the average intensity value "U" and standard deviation "σ" are defined as follows:

$$U = \frac{1}{m\times n}\sum_{i=1}^{m}\sum_{j=1}^{n}W(i,j), \tag{8}$$

$$\sigma = \sqrt{\frac{\sum_{i=1}^{m}\sum_{j=1}^{n}(W(i,j)-U)^2}{m\times n}}, \tag{9}$$

where "$W(i,j)$" is the function of the new image, whose size is "$m \times n$".

Secondly, the intensity threshold value "T" of the new image is computed by

$$T = U + c * \sigma. \tag{10}$$

The symbol "c" is a control constant. In this study, after measurements of 200 times, we used $c = -1$.

As shown in Fig. 4, the pixel amplitudes of seams or stitching defects are lower than those of normal places, the thresholding processing is defined as:

$$g(i,j) = \begin{cases} 1 & \text{if } h(i,j) \leqslant T, \\ 0 & \text{if } h(i,j) \geqslant T, \end{cases} \tag{11}$$

where "$g(i,j)$" has the same size as "$h(i,j)$".

There normally exists noise in the thresholded results. It is noted that noise in the detection results appears as isolated small regions whose area is much smaller than that of defect regions. In this study, mean filtering of size 3×3 was used as a post-processing step.

3.2. Defect classification

An important aim of this study is to classify the detected stitching defects into different categories. Firstly, image features belonging to the defective regions were extracted. A BP neural network can train multilayer feed-forward networks with differentiable transfer functions to perform pattern classification. Hence, BP neural network was employed to classify the stitching defects.

3.2.1. Feature extraction

After the stitching defect segmentation, the binary image is generated. The next step is to extract the features of stitching areas for further computer processing. Most of the stitches show the directionality of periodic patterns in an image, just like the texture. An important approach used for describing a region is to quantify its texture content. Two methods employed for computing texture are statistical approach and spectral measure (Gonzalez & Wood,

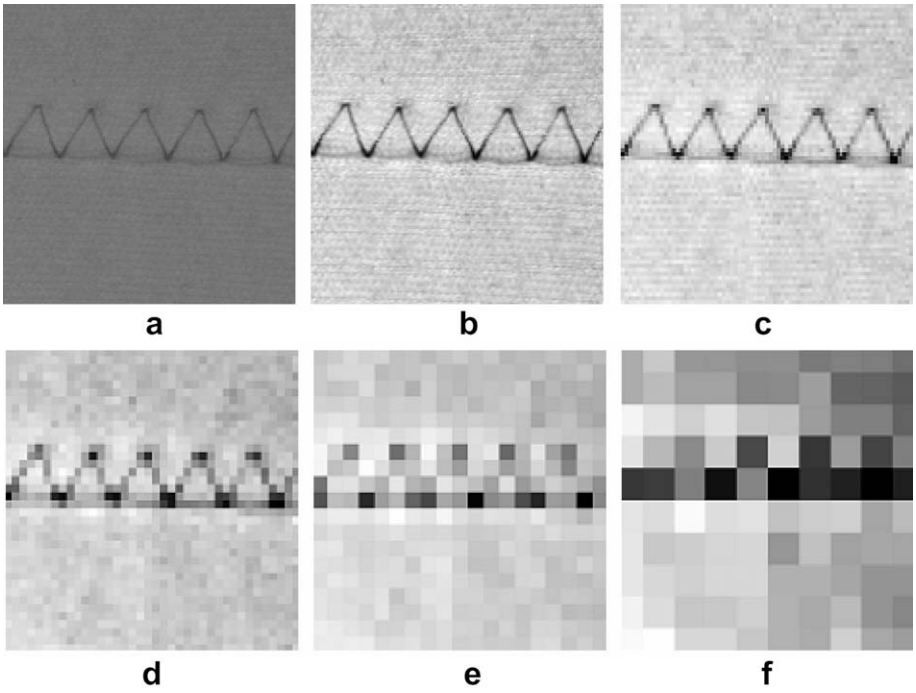

Fig. 6. The effect of varying levels of wavelet transform: (a) the original image with stitching defects; (b)–(f) the decomposition smooth images from multiresolution levels $j = 1,2,\ldots,5$.

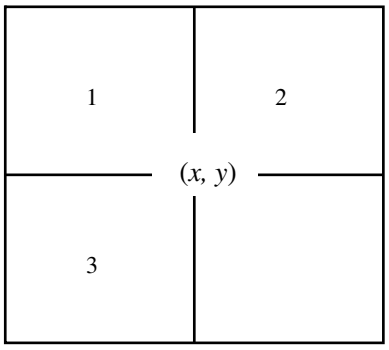

Fig. 7. Quadrant mean filter method.

2002). In this study, the spectral measure of texture was used based on the Fourier spectrum suitable for describing the directionality of periodic or almost periodic 2-D patterns in an image. Spectral techniques are used primarily to detect the periodicity in an image by identifying high energy and narrow peaks in the spectrum.

Detection and interpretation of the spectral features are simplified by expressing the spectrum in polar coordinates to yield a function "$S(r,\theta)$", where "S" is the spectrum function while frequency "r" and direction "θ" are the variables in this coordinate system. For each frequency"r", "$S(r,\theta)$" is considered as a 1-D function "$S_\theta(r)$". Analyzing "$S_\theta(r)$" for a fixed value of "θ" yields the behavior of the spectrum along a radial direction from the origin. Analyzing "$S_r(\theta)$" for a fixed value of "r" yields the behavior along a circle centered at the origin. By summing up these functions, a global description is obtained:

$$S(r) = \sum_{\theta=0}^{\pi} S_\theta(r), \tag{12}$$

$$S(\theta) = \sum_{r=1}^{R_0} S_r(\theta), \tag{13}$$

where "R_0" is the radius of a circle centered at the origin.

Two 1-D functions, "$S(r)$" and "$S(\theta)$" constitute a spectral-energy description of texture for an entire image or region under consideration. Some descriptors of the function "$S(\theta)$" can be calculated in order to characterize their behavior quantitatively. Descriptors used for this purpose are the (1) maximum value, (2) minimum value, (3) distance between the former two values, (4) mean, (5) standard deviation, (6) and (7) other maximum values in the fields segmented by the maximum value (the number is two), and (8) and (9) offsets between the other maximum values and minimum values which are both in the segmented fields (the number is two). Totally, nine characteristic variables of $S(\theta)$ are obtained.

The values of the nine characteristic variables are not at the same quantitative level and the ranges of their values are also dif-

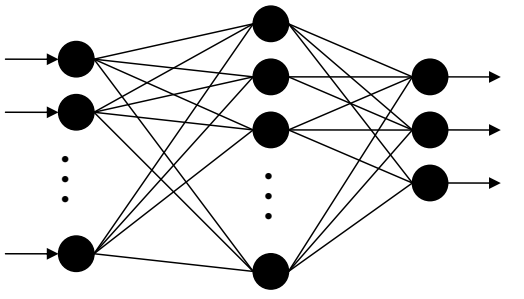

(a) the architecture of the BP Neural network

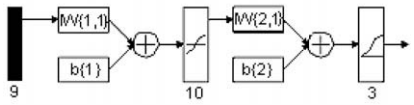

(b) the layer diagram of the BP Neural network

Fig. 8. BP neural network architecture and layer diagram.

ferent. These differences influence the representation of each class of stitching defects. To produce the most efficient training, the data are preprocessed before training and need to be processed in uniform measurement. Another reason for preprocessing the data is that when the input variables of a sigmoid function are in the range of [−1,1], the distances of the outputs are very different, which is useful for classification and recognition.The data preprocessing is expressed as follows:

$$Y = \frac{y - \bar{y}}{y_{\max} - y_{\min}}\beta, \tag{14}$$

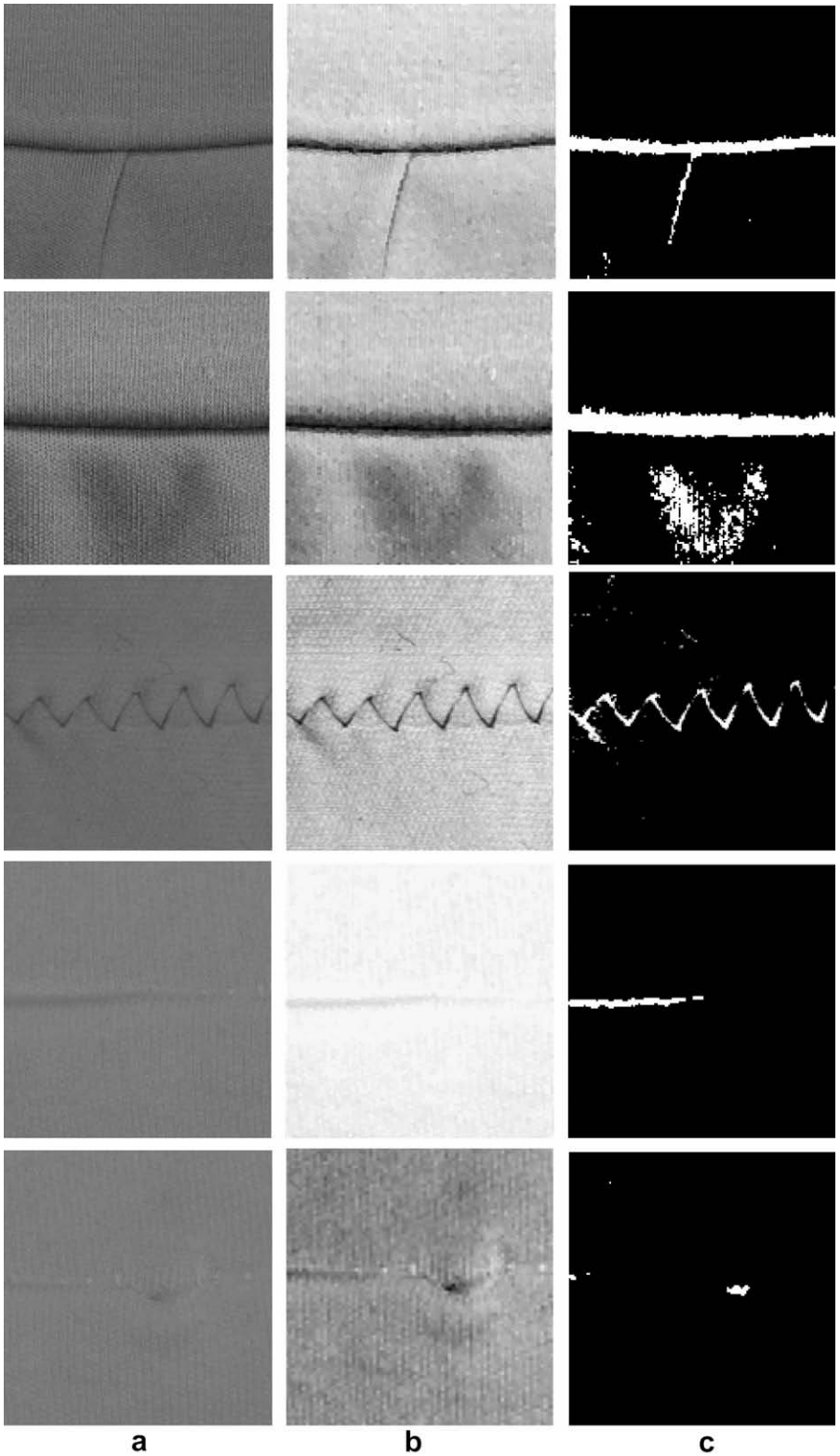

Fig. 9. Detection of the five types of stitching defective images: (a) the original images, (b) the quadrant mean filtered images, and (c) the binary images after thresholding and noise filtering.

where the symbol "Y" is the relative characteristic value, "y" is the absolute characteristic value, "$\bar{y}$" is the mean of "y", "y_{max}" and "y_{min}" are the maximum and the minimum values of "y".

3.2.2. Defect classification based on the BP neural network

In general, a BP network is multilayer, fully connected and feed-forward. The first and last layers are called the input and output layers. The layers between the input and output layers are called the hidden layers. Input vectors and the corresponding target vectors are used to train a BP network to develop internal relationships between nodes so as to organize the training data into classes of patterns. This same internal representation can be applied to inputs that are not used during training. The trained BP network tends to give reasonable answers when presented with inputs that the network has never seen. This generalization property makes it possible to train a network on a representative set of input/target pairs and get good results without training the network on all possible input/output pairs.

In this study, a two-layer BP neural network was designed and the architecture is illustrated in Fig. 8a. The network is formulated as a two-layer tangent sigmoid/log sigmoid network in which the log sigmoid transfer function is employed since its output range is perfect for learning the output bipolar values, i.e. 0 and 1, as shown in Fig. 8b. There are nine characteristic variables of the directional function "$S(\theta)$", yielded from any of the classified images obtained by the method of texture spectral measure. The number of neural nodes of the input layer is nine corresponding to the nine characteristic valuables. The number of neural nodes of the output layer is three so that the output values, i.e. 000, 001, 010, 011 and 100, corresponding to the five classes of stitching defective images. The number of hidden layers is ten, which is confirmed by testing. The training function of the BP neural network is a gradient descending function based on a momentum and an adaptive learning rate. The learning algorithm of the connection weights and the threshold values is a momentum-learning algorithm based on gradient descending.

4. Experimental results

In this section, the experimental results are presented to evaluate the performance of the proposed method. Samples of five types of common stitching defects in apparel manufacture, which are listed in Fig. 4, were used for experimental testing. All images were collected by a common digital camera and had 300×300 pixels and 256 gray levels. Throughout the experiments, the Daubechies wavelet was used for all testing samples and the images were decomposed at level 1.

4.1. Stitching defect detection

The energies of the wavelet coefficients distributed in low–low frequency channels provide the most important information about the stitches. The smooth subimage with the attenuating texture background was chosen for the following process. Due to the multiresolution property in the wavelet transform, $m+1$ level has a lower resolution than m level. For the level 1 Daubechies wavelet transform, the subimage is of resolution of 2×2 blocks. Hence, each stitch is larger than or around 2×2 pixels of the original image. Defects with a size smaller than 2×2 pixels may not be detected.

Fig. 9a shows the images including a stitch embedded in the fabric texture. The smoothed images are obtained by applying the wavelet transform and the quadrant mean filter as given in Section 3 and shown in Fig. 9b. Thresholding is applied to localize the stitch region and remove the background. The stitch regions are well detected and located from the binary image as shown in Fig. 9c. In the experimental study, the proposed method was used to test five different stitching defective regions that involved 200 images of varied defects. The success rate of detection was 100%.

For comparisons of the proposed method with the direct thresholding method and with the automatic band selection for the wavelet reconstruction method, the experiment as shown in Fig. 10 is conducted. Most energies concentrated on the smooth

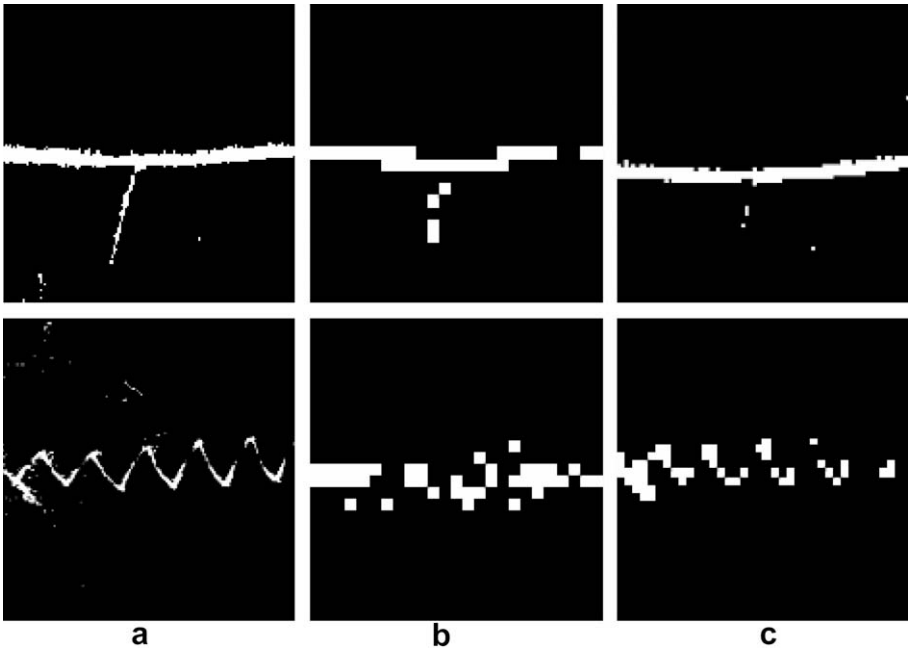

Fig. 10. Experimental results of (a) the proposed method; (b) the direct thresholding method and (c) the automatic band selection for wavelet reconstruction method.

image and provides the most important information about the stitches among the four decomposed subimages and the smooth subimage was used for defect detection. As there is a lot of shadow noise in these images caused by the illumination environment, the quadrant mean filter was used to improve the stitching defect detection efficacy overcoming the drawback of the other two methods. In our study, the stitching defect is a very thin anomaly in the fabric textural background, and the high level of the wavelet transform selected in the two aforementioned methods could not yield good performance in outlining the stitching defects. Experimental results show that the proposed method gives more exact segmentation results than the other two methods.

4.2. Stitching defect classification

Feature extraction is a key step for the classification. The method of texture spectral measure to obtain the nine features is used and the spectral measure results are presented in Fig. 11. The figure shows that there are great differences in the spectral measure results among the five classes of stitching defects. The features decrypted by the spectral measure are effective.

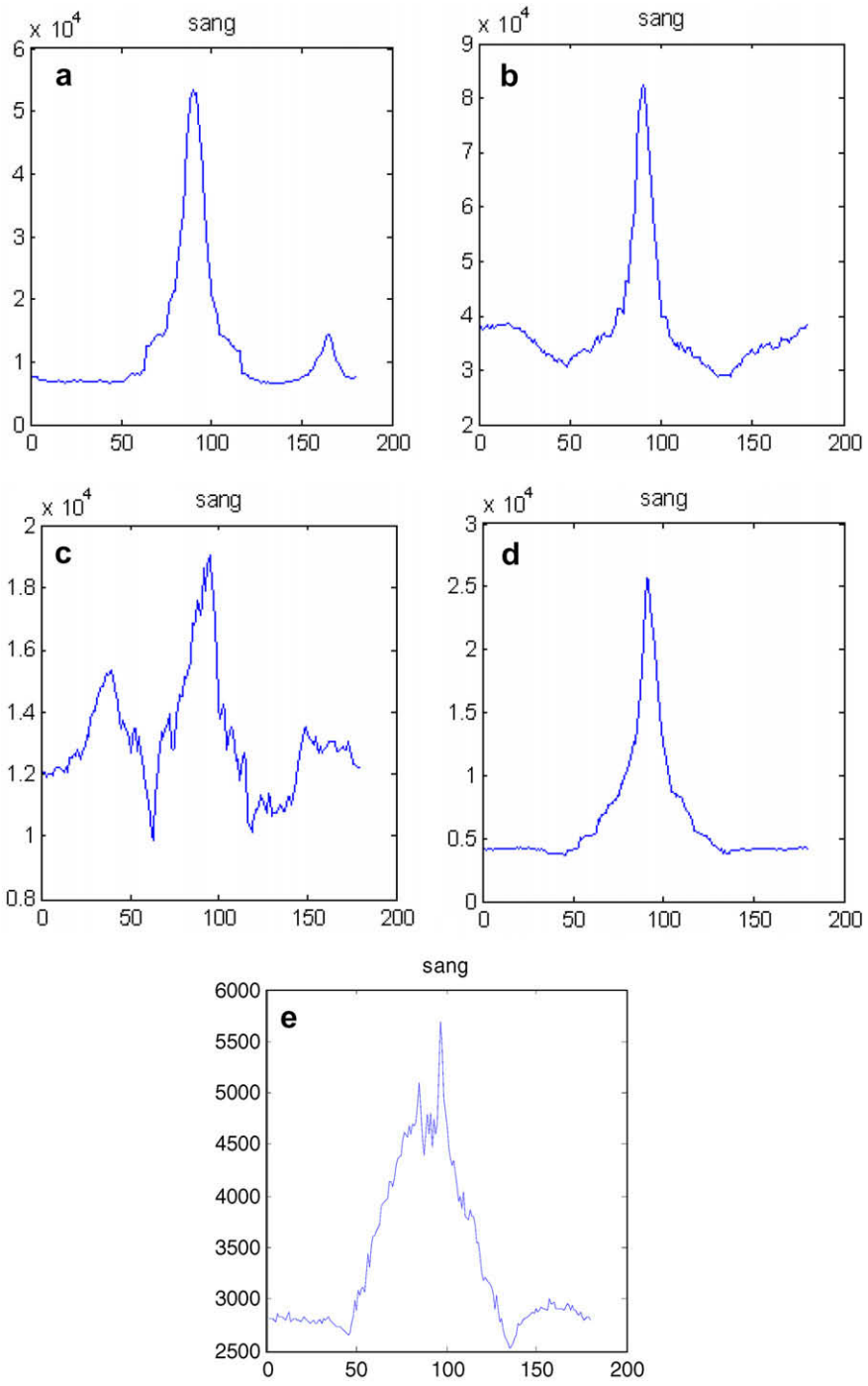

Fig. 11. Plots of function "$S(\theta)$" of the five classes: (a) D1, (b) D2, (c) D3, (d) D4 and (e) D5.

Table 2
Classification results with the BP neural network

Stitching defects	Correct classification rate
D1	100%
D2	100%
D3	100%
D4	100%
D5	93%

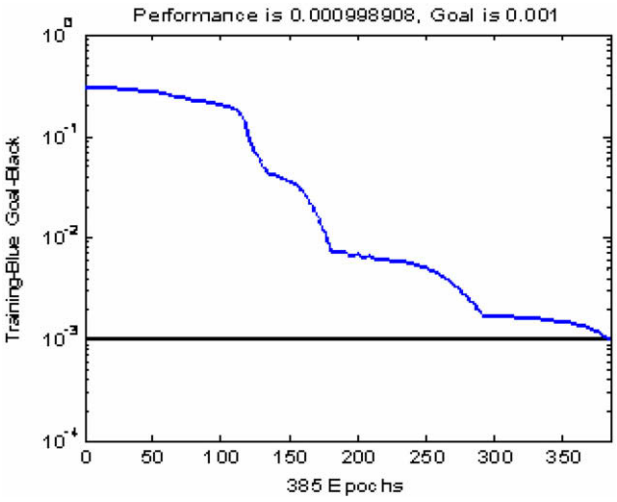

Fig. 12. Training curve of the BP neural network.

In this experiment, a two-layer feed-forward network trained with the back propagation (BP) is used. The network received a 9-element input vector in order to identify the class by responding to a 3-element output vector representing five classes of site suitability. A tangent function between the input and hidden layers and a logarithmic function between the hidden and output layers were used. The hidden layer had 10 neurons after the trial test.

Table 2 demonstrates the performance of the BP neural network classification algorithm. The percentage shown in the table represents the number of correct classification times out of 1000 trials in which random initial weights were used in each trial. In each trial, the network was trained until the squared error was less than 0.000001.

The training curve denoting the training procedure is shown in Fig. 12. The curve is convergent when the training goal describing the error between the training output and the ideal output is defined as 10^{-3}, and the goal is reached at 401 epochs in this training procedure. Therefore, the result of the training procedure is satisfactory.

5. Conclusions

In this study, a fabric stitching hybrid approach using the wavelet-based method to detect stitching defects in the fabric image and a two-layer BP neural network is proposed to classify the detected defects. Experiments conducted on the five classes of images of stitching defects yield satisfactory results. The proposed method shows high recognition and detection accuracy in the detection and classification of stitching defects.

Experiments were conducted to compare the improved direct thresholding method with the direct thresholding method based on wavelet transform detailed subimages and the automatic band selection for the wavelet reconstruction method. In this study, it was found that over 95% of energies concentrated on the smooth image and the energies provide the most important information about the stitches among the four decomposed subimages. The smooth subimage with the attenuating texture background was chosen for further processing. As the dimension of stitching defects are very thin, the thresholding method based on single resolution level wavelet transform leads to better results. The quadrant mean filter can further attenuate the background and accentuate the stitching defects. The results demonstrate that the proposed method outperforms the other two wavelet-based methods.

Acknowledgements

The authors would like to thank Earmarked Research Grant of Research Grants Council of Hong Kong and The Hong Kong Polytechnic University for the financial support in this research project (Project code: PolyU 5313/05E).

References

Amet, A. L., Ertuzun, A., & Ercil, A. (1998), Texture defect detection using subband domain co-occurrence matrices. In *IEEE southwest symposium on image analysis and interpretation* (pp. 205–210).
Arivazhagan, S., & Ganesan, L. (2003). Texture segmentation using wavelet transform. *Pattern Recognition Letters, 24*(16), 3197–3203.
Bovik, A. C., & Clark, M. (1990). Multichannel texture analysis using localized spatial filters. *IEEE Transactions on Pattern Analysis and Machine Intelligence, 12*(1), 55–73.
Chang, T., & Kuo, C. C. (1993). Texture analysis and classification with tree-structured wavelet transform. *IEEE Transactions on Image Process, 2*(4), 429–440.
Chan, C. H., & Pang, G. K. H. (2000). Fabric defect detection by Fourier analysis. *IEEE Transactions on Industry Applications, 36*(5), 1743–1750.
Chitre, Y., & Dhawan, A. P. (1999). M-band wavelet discrimination of natural textures. *Pattern Recognition, 32*(5), 773–789.
Coggins, J. M., & Jain, A. K. (1989). A spatial filtering approach to texture analysis. *Pattern Recognition Letters, 3*(3), 195–203.
Cohen, F. S., Fan, Z., & Attai, S. (1991). Automated inspection of textile fabrics using textural models. *IEEE Transactions on Pattern Analysis Machine Intelligence, 13*(8), 803–808.
Dorrity, J. L., Vachtsevanos, G., & Jasper, W. (1996). Real-time fabric defect detection and control in weaving processes. National Textile Center Annual Report (pp. 113–122). Wilmington, DE.
Gonzalez, R. C., & Wood, R. E. (2002). *Digital image processing* (2nd ed.). Upper Saddle River, NJ: Prentice Hall.
Gupta, L., & Sortrakul, T. (1998). A Gaussian-mixture-based image segmentation algorithm. *Pattern Recognition, 31*(3), 315–325.
Jain, A. K., & Farrokhnia, F. (1991). Unsupervised texture segmentation using Gabor filters. *Pattern Recognition, 24*(12), 1167–1186.
Jasper, W., Joines, J., & Brenzovich, J. (2005). Fabric defect detection using a genetic algorithm tuned wavelet filter. *Journal of The Textile Institute, 96*(1), 43–54.
Jiang, S.-S., & Sawchuk, A. A. (1986). Noise updating repeated Wiener filter and other adaptive noise smoothing filters using local image statistics. *Applied Optics, 25*(14), 2326–2337.
Kim, S. C., & Kang, T. J. (2007). Texture classification using wavelet packet frame and Gaussian mixture model. *Pattern Recognition, 40*(4), 1207–1221.
Lu, C. S., Chung, P. C., & Chen, C. F. (1997). Unsupervised texture segmentation via wavelet transform. *Pattern Recognition, 30*(5), 729–742.
Mallat, S. G. (1989). A theory for multiresolution signal decomposition: The wavelet representation. *IEEE Transactions on Pattern Analysis Machine Intelligence, 11*(7), 674–693.
Mallat, S. (1999). *A wavelet tour of signal processing* (2nd ed.). San Diego: Academic Press.
Ngan, Y. T., Pang, K. H., Yung, S. P., & Ng, K. (2005). Wavelet based methods on patterned fabric defect detection. *Pattern Recognition, 38*(4), 559–576.
Pyun, K., Lim, J., Won, C. S., & Gray, R. M. (2007). Image segmentation using hidden Markov Gauss Mixture models. *IEEE Transactions on Image Processing, 16*(7), 1902–1910.
Sari-Saraf, H., & Goddard, J. Jr., (1999). Vision system for on-loom fabric inspection. *IEEE Transactions on Industry Applications, 36*(6), 1252–1258.
Sengur, A. (2007). Wavelet transform and adaptive neuro-fuzzy inference system for color texture classification. *Expert Systems with Applications*. doi:10.1016/j.eswa.2007.02.032.
Song, X. F., Chen, Z. G., Wen, C. L., & Ge, Q. B. (2003). Wavelet transform-based texture segmentation using feature smoothing. In *Proceedings of the second international conference on machine learning and cybernetics* (pp. 2370–2373).
Tsai, D. M., & Chiang, C. H. (2003). Automatic band selection for wavelet reconstruction in the application of defect detection. *Image and Vision Computing, 21*(5), 413–431.

Tsai, I. S., & Hu, M. C. (1996). Automatic inspection of fabric defects using an artificial neural network technique. *Textile Research Journal, 66*(7), 474–482.

Tsai, D. M., & Huang, T. Y. (2003). Automated surface inspection for statistical textures. *Image and Vision Computing, 21*(4), 307–323.

Unser, M. (1995). Texture classification and segmentation using wavelet frames. *IEEE Transactions on Image Processing, 4*(11), 1549–1560.

Vangheluwe, L., Sette, S., & Pynckels, F. (1993). Assessment of set marks by means of neural nets. *Textile Research Journal, 63*(4), 244–246.

Yang, X. Z., Pang, G., & Yung, N. (2002). Fabric defect classification using wavelet frames and minimum classification error training. In *Industry applications conference, 37th IAS annual meeting* (Vol. 1, pp. 290–296).

Yang, X. Z., Pang, G., & Yung, N. (2004). training approaches to fabric defect classification based on wavelet transform. *Pattern Recognition, 37*(5), 889–899.

Zhang, Y. F., & Bresee, R. R. (1995). Fabric defect detection and classification using image analysis. *Textile Research Journal, 65*(1), 1–9.